Magn Reson Med Sci, Vol. 7, No. 3, pp. 131–140, 2008

MAJOR PAPER

Production of a Human-Tissue-Equivalent MRI Phantom: Optimization of Material Heating

Seiichiro OHNO[1,2]*, Hirokazu KATO[2], Takashi HARIMOTO[2,3], Yusuke IKEMOTO[2], Keisuke YOSHITOMI[2], Sigefumi KADOHISA[1], Masahiro KURODA[2], and Susumu KANAZAWA[4]

[1]*Central Division of Radiology, Okayama University Hospital*
2–5–1, Shikata-cho, Okayama-shi, Okayama 700–8558, Japan
[2]*Graduate School of Health Sciences, Okayama University*
[3]*Department of Radiology, Kitagawa Hospital*
[4]*Graduate School of Medicine, Dentistry and Pharmaceutical Sciences, Okayama University*
(Received January 15, 2008; Accepted July 2, 2008)

Purpose: We conceived a 2-stage heating method to dissolve the ingredients of magnetic resonance (MR) imaging phantoms to overcome issues of uneven quality in conventional MR imaging phantoms, and we evaluated uniformity and the reproducibility of our method.

Methods: We used a 3-liter capacity, column-shaped, enamel-coated porcelain container to produce a muscle-equivalent phantom (diameter, 160 mm; height, 100 mm; volume, 2 liters). The phantom contained: 1) carrageenan as a gelling agent; 2) agarose as a T_2 modifier; 3) $GdCl_3$ as a T_1 modifier; 4) NaN_3 as an antiseptic; and 5) distilled water. We applied both direct heating and 2-stage heating of pre-soaked materials. We placed powdered materials directly into hot water for direct heating but soaked them in water one day before use (post-swelling) in 2-stage heating. The materials in the container were melted in a silicone oil bath of 120 or 140°C under various conditions, then allowed to gel by natural cooling. We observed the resulting gel phantoms macroscopically using a CCD camera and evaluated their uniformity by microscopy and MR imaging.

Results: We found it necessary to raise the temperature inside the phantom to 100.0°C, to produce a uniform gel with stable homogeneity and few bubbles. Use of an enamel-coated porcelain container required setting the temperature of the oil bath at 140°C.

Conclusion: A uniform and reproducible human tissue-equivalent phantom with few bubbles can be manufactured using our 2-stage heating method, which employs pre-soaking in a silicone oil bath at 140°C for 30 min. We then added the swollen carrageenan to the agarose solution, which heating the temperature to 140°C for 30 min while continuously stirring at 120 rpm, following with natural cooling.

Keywords: ***MRI phantom, oil bath, production method, homogeneity, reproducibility***

Introduction

Phantom measurement is essential for various magnetic resonance (MR) imaging applications, such as testing of equipment performance, correction of image quality and contrast, evaluation of new pulse sequences, adjustment of operational conditions, technical training of operators, simulation of specific organ visualization, and for use in various studies.[1–27] A human tissue-equivalent phantom is also useful in evaluating safety. In experimental MR imaging research, result reliability depends on the phantom used. A human tissue-equivalent MR imaging phantom requires: 1) human tissue-equivalent relaxation time; 2) human tissue-equivalent electrical conductivity; 3) uniform relaxation time and electrical conductivity over the entire phantom; 4) shape-retaining strength without reinforcement; 5) capacity to be shaped into forms similar to those of human organs; 6) easy preparation; and 7) no deterioration of quality over a long period.[28]

To date, MR imaging phantoms have been either

*Corresponding author, Phone: +81-86-223-7151, Fax: +81-86-235-7723, E-mail: ohno_s@hp.okayama-u.ac.jp

liquid or gels. Liquid phantoms include aqueous solutions of paramagnetic ions, such as $CuSO_4$ and $NiSO_4$.[1,2] Gel phantoms include polysaccharide gels, such as agarose and agar;[3–15] protein gels, such as gelatin;[16–19] polyvinyl alcohol (PVA) gels;[20–23] polyacrylamide gels;[24–26] and silicone gels.[27] Liquid phantoms containing paramagnetic ions are typically used to evaluate equipment performance, but liquid phantoms are not human tissue-equivalent and cannot retain their shapes without use of a container. When polysaccharide gels or protein gels are used to prepare a tissue-equivalent phantom with a long T_2 relaxation time, the density becomes too low to maintain satisfactory strength. Preparation of PVA, polyacrylamide, or silicone gels is time-consuming and costly, and their sizes and shapes cannot be easily changed.

We developed an MR imaging phantom containing carrageenan, agarose gadolinium chloride, and sodium chloride, which we called a ''CAGN phantom'',[28–31] that overcomes the above shortcomings. We conducted basic experiments with small amounts of phantom material, but for clinical applications, a larger phantom was desired.

In this study, we prepared a cylindrical muscle-equivalent phantom measuring 160 mm$\phi \times$100 mmh, which is applicable for MR imaging using a head coil. Prior to this study, the dissolution of carrageenan and agarose powders, which are primary phantom materials, were tested using a bath of either hot water or hot saline solution to reach high temperatures. However, the temperature of the solution in a stainless steel container did not reach dissolution temperature, so dissolution was uneven. Dissolution using a glass container heated using an infrared heater produced a scorched sample, and dissolution was poor after placing a glass container in an oil bath at constant temperature because of the low thermal conductivity of the glass container. Although the thermal conductivity of stainless steel containers is better than that of glass containers, elution of metal ions from the containers was anticipated during heating at high temperatures.

In this study, to achieve higher temperatures inside the container and avoid scorching of phantom materials, we used a silicone oil bath with an enamel-coated porcelain container, and we evaluated the quality and stability of this method.

Materials and Methods

Equipment

To prepare the phantom, we used: an oil bath (BOA310: Yamato Scientific Co., Ltd., Tokyo, Japan); silicone oil (SRX310: Toray, Tokyo, Japan); a stirrer (NZ–1200: Tokyo Rikakikai Co., Ltd., Tokyo, Japan), and an enamel-coated porcelain container (columnar shape, 160-mm diameter, 3-liter capacity) (Fig. 1).

For measurement, we used: an electromagnetic balance (GX–2000: A&D Co., Ltd., Tokyo, Japan); an electronic balance (CP34001P: Sartorius AG, Germany); a digital thermometer (TM–305: A.S. One Co., Ltd., Sendai, Japan); an optical microscope (Axiophoto FL: Carl Zeiss Inc., Germany); a CCD camera (HC–200: Fujifilm Co., Tokyo, Japan); MR equipment (1.5T Magnetom Vision: Siemens, Erlangen, Germany); a CP-head coil; and image analysis software (Image J: National Insti-

Fig. 1. Phantom preparation equipment. (**a***: entire view,* **b**: top view) An oil bath with silicone oil (340 × 293 × 270 mm), an enamel-coated porcelain container (diameter: 160 mm; capacity: 3 liters), and a mixer. In Fig. 1b, 2 liters of materials are heated.

tutes of Health [NIH], USA).

Phantom materials

1. Phantom components. The phantom was composed of carrageenan (fixed at 3%) (KC–200S: Chuo Kasei Co., Ltd., Osaka, Japan) as a gelling agent; $GdCl_3$ (Katayama Chemical, Osaka, Japan) as a T_1 modifier; agarose (Type 1, #A–6013: Sigma Chemical Corp., St. Louis, MO, USA) as a T_2 modifier; NaCl (Katayama Chemical, Osaka, Japan) as an electrical conductivity modifier; NaN_3 (fixed at 0.03%) (Katayama Chemical, Osaka, Japan) as an antiseptic; and distilled water.

2. Calculation of components for a 2-L muscle-equivalent phantom. For MR imaging, the recognized relaxation times and electrical properties of the muscle in a 1.5T unit have been: T_1 value, 867 ms; T_2 value, 47 ms; and electrical conductivity, 0.688 S/m.[31] The corresponding values for our phantom components were determined based on the literature[31] and included 3% carrageenan, 38.7 μmol/kg $GdCl_3$, 1.413% agarose, 0.277% NaCl, 0.03% NaN_3, and distilled water. To prepare a 2,000-g muscle-equivalent phantom, then, we used 60 g of carrageenan, 7.75 g of $GdCl_3$, 28.26 g of agarose, 5.53 g of NaCl, 0.6 g of NaN_3, and 1,897.86 g of water. These components were dissolved and then solidified into a columnar-shaped gel measuring 160 mmϕ × 100 mmh.

Experimental Methods

Production of phantom

We made a columnar muscle-equivalent phantom of 160 mmϕ × 100 mmh as follows:

1. Temperature of materials. According to the literature,[32,33] agarose dissolves at 90–100°C and gels at 40°C, whereas carrageenan dissolves at 70°C or higher and gels at 60°C. In our preliminary experiments, we confirmed that when the temperature inside the container was lower than 100°C, the dissolution of agarose was poor, and insoluble clusters occurred. In this study, to ensure that the temperature inside the container reached 100°C, we dissolved the agarose using an oil bath.

2. Temperature of oil bath and heating time. We investigated the relationship between the temperature of the oil bath and that inside the container. We mixed all components for the muscle-equivalent phantom and poured them into the container, set the oil bath temperature to either 120 or 140°C, and placed the container into the bath at a room temperature of 25 ± 1°C. We measured the temperature inside the container using a digital thermometer. From the data obtained, we made temperature-time curves that indicated the time necessary to raise the temperature in the container to 100°C.

3. Direct dissolution method. First, we placed a container with water of room temperature into a hot oil bath. When the water started to boil, we put all powder components of the phantom into the boiling water and stirred at 120 rpm using a stirrer. The solution was then naturally cooled to allow degassing and solidification into gel.

4. Two-stage heating method using pre-soaked materials. One day before the experiment, we placed powdered carrageenan; agarose containing $GdCl_3$; NaCl; and NaN_3 into distilled water of room temperature to soak and swell. The swollen components were heated and dissolved on the day of experiment.

The 2-stage heating procedure consisted of initially placing an enamel-coated porcelain container with swollen agarose into an oil bath at 140°C and stirring the agarose solution at 120 rpm. Heating continued for 30 min, while the temperature inside the container reached 100.0°C. We then added the swollen carrageenan to the agarose solution, which reduced the temperature inside the container, and continued stirring for another 30 min. After a total of 60 min heating, the solution was allowed to solidify into a gel by natural cooling.

Evaluation of phantoms (direct dissolution versus 2-stage heating method using pre-soaked materials):

1. MR imaging evaluation. We evaluated the phantoms using MR imaging with the spin-echo (SE) and gradient-echo (GRE) methods at room temperature of 25 ± 1°C and parameters generally applied for clinical imaging of the head using a head coil. SE parameters were: repetition time/echo time (TR/TE) = 450 ms/14 ms; flip angle = 70°; slice thickness = 10 mm; transverse orientation; matrix = 512 × 512; field of view (FOV) = 220 mm; number of excitations (NEX) = 2; band width = 89 Hz/pixel; and scan time = 7 min 44 s. GRE parameters were: TR/TE = 450 ms/15 ms, flip angle = 15°, slice thickness = 10 mm, transverse orientation, matrix = 512 × 511, FOV = 220 mm, NEX = 2, bandwidth = 78 Hz/pixel, and scan time = 7 min 42 s.

2. Microscopic evaluation. To observe the dissolution state, we observed 1.5-mm-thick slices of the phantom using an optical microscope at 50-times magnification.

Evaluation of reproducibility in a 2-stage heating method using pre-soaked materials:

To confirm the reproducibility of the phantom

production method, we prepared 2 phantoms (Phantoms 1 and 2) on separate days. We made these phantoms by combining the post-swelling dissolution and the 2-stage heating methods. Because water evaporation causes weight loss during phantom preparation, we added 200 g of water beforehand to achieve a phantom weighing 2,000 g.

1. T_1 and T_2 values of MR imaging. We measured the T_1 and T_2 values of the 2 phantoms to confirm reproducibility. Measurements were carried out by SE, as previously reported.[28] The parameters were: slice thickness = 10 mm; orientations = transverse, coronal, and sagittal; matrix = 256 × 256; FOV = 220 mm; NEX = 1; and bandwidth = 130 Hz/pixel.

T_1 values were measured at a fixed TE (15 ms) and various TR values (140, 175, 232, 309, 410, 545, 724, 962, 1,699, 3,000, 5,287, 9,332, and 16,474 ms). T_2 values were measured at a fixed TR (10,000 ms) and various TE values (15, 22, 29, 39, 52, 69, 93, 125, 167, 224, and 300 ms). As shown in Fig. 2, we measured T_1 and T_2 values at 5 regions of interest (ROI) (O, A, B, C, and D), each of which measured 13.1 cm^2.

2. Uniformity. We measured phantom uniformity according to the method of the National Electrical Manufacturers Association (NEMA).[34] In addition to the subject columnar phantoms, we used another spherical-shaped phantom (diameter, 170 mm) containing aqueous nickel sulfate solution as a control to measure uniformity. For evaluation, we placed an ROI with an area of 141.9 cm^2 on SE-MR images and measured the maximum (Smax) and minimum (Smin) pixel values in the ROI. We detemined the span (Δ) by the formula (Smax − Smin)/2 and the median value (S), by (Smax + Smin)/2. Uniformity (U) was determined by the formula $\pm 100 \times (\Delta/S)$[%]. Imaging conditions for the SE method were: TR/TE = 500 ms/15 ms, flip angle = 90°, slice thickness = 5 mm, transverse orientation, matrix = 256 × 256, FOV = 180 mm, NEX = 1, bandwidth = 130 Hz/pixel, and scan time = 2 min 11 s.

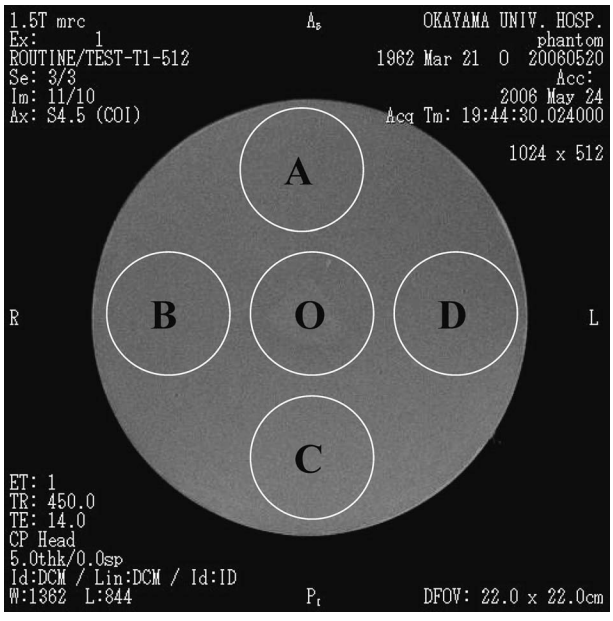

Fig. 2. Five regions of the columnar phantom on an MR image (transverse slice) for measuring T_1 and T_2 values.

3. Bubbles. We evaluated bubbles in the phantom based on the number of bubble pixels on GRE-MR images. The GRE method is considered sensitive to differences in magnetic susceptibility. We imaged a columnar-shaped region (diameter 60 mm) in the center of the phantom, and the section was continuously sliced into 20 images of 3-mm thickness without gaps. One slice of the phantom (diameter 160 mm) contained approximately 109,000 pixels. The obtained image data were digitized using ''Image J'' software, and areas of low signal intensity (black color) containing 5 pixels or more were regarded as bubbles.

Imaging parameters for measuring bubbles were: TR/TE = 640 ms/15 ms, flip angle = 15°, slice thickness = 3 mm, number of slices = 20, slice gap = gapless, transverse orientation, matrix = 512 × 512, FOV = 220 mm, NEX = 2, bandwidth = 78 Hz/pixel, and scan time = 10 min 56 s.

Statistical examination:

We used unpaired Student's t-test to evaluate property differences between phantoms based on the mean and standard deviation for each ROI in ''Experimental Methods: 1. T_1 and T_2 values of MR imaging'' and Mann-Whitney's U test to analyze results from ''Experimental Methods: 3. Bubbles.''

Results

Production of phantom

1. Temperature and heating time. Figure 3 shows the temperature rise inside the container when the temperature of the oil bath was set at 120 or 140°C. When the temperature of the bath was set at 120°C, the temperature inside the container was 99.8°C, even 60 min after the start of heating. When the temperature of the oil bath was set at 140 °C, the temperature inside the container reached 100.0°C within 30 min after the start of heating.

2. Direct dissolution method. MR images of the phantoms prepared by the direct dissolution method are shown in Fig. 4. On the SE image (Fig. 4a), we saw numerous spots of low concentration with

diameters approximately 2 mm. On the GRE image (Fig. 4b), we saw numerous spots of low concentration with diameters approximately 5 mm. Figure 5 shows an optical micrograph of the phantom. We observed numerous clusters caused by poor dissolution.

3. Two-stage heating method using pre-soaked materials. Figure 6 shows MR images of the phantom prepared by combining the post-swelling dissolution and the 2-stage heating methods. On the SE image (Fig. 6a), no bubbles were observed in the phantom. On the GRE image (Fig. 6b), however, 2 or 3 bubbles of approximately 1 mm were seen. Figure 7 shows an optical micrograph of the phantom. No clusters were observed.

Phantom properties in a 2-stage heating method using pre-soaked materials:

The resultant weights of the 2 columnar-shaped phantoms were 1993.8 g (Phantom 1) and 2016.5 g (Phantom 2) (mean weight, 2005.2 ± 11.3 g).

1. T_1 and T_2 values of MR imaging. To evaluate the reproducibility of phantom preparation, we compared variations in the T_1 and T_2 values in Phantoms 1 and 2. Tables 1 and 2 show the T_1 and

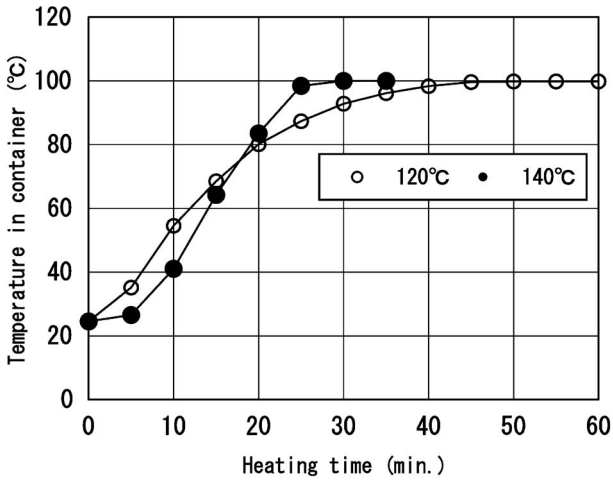

Fig. 3. Temperature inside the phantom container relative to the temperature of an oil bath.

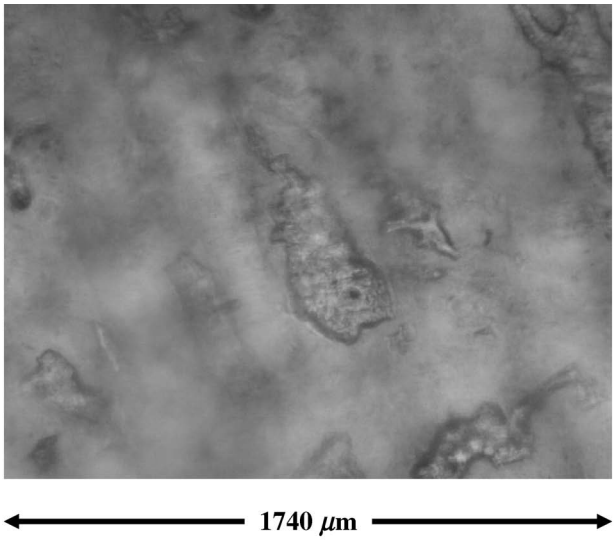

Fig. 5. Optical micrograph of a phantom prepared by the direct dissolution method (magnification: 50 times).

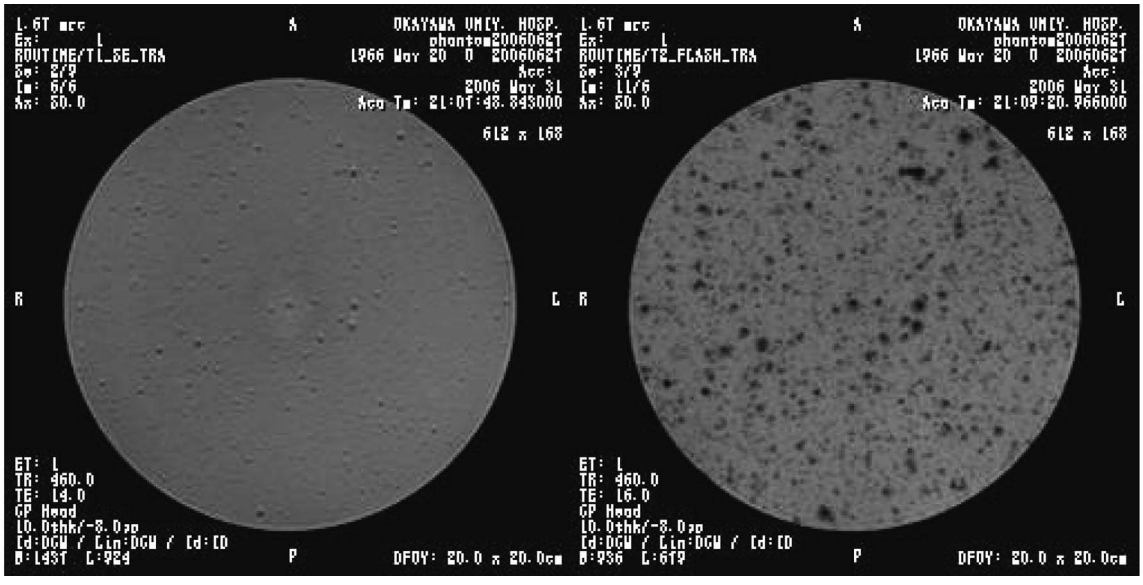

Fig. 4. Magnetic resonance (MR) images of a phantom prepared by the direct dissolution method. **a**: spin-echo (SE) image, **b**: gradient-echo (GRE) image.

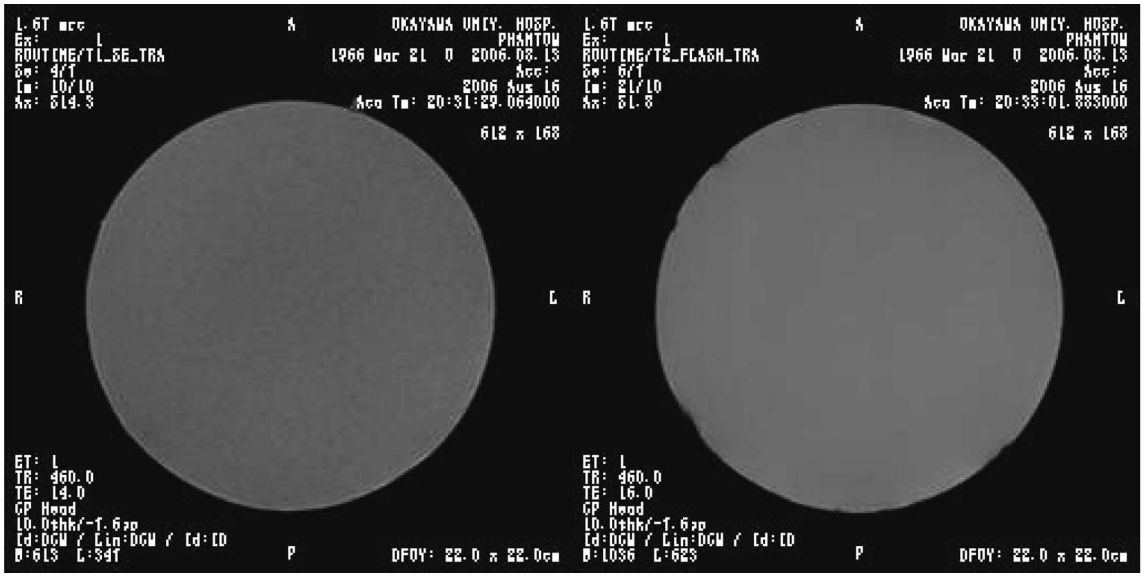

Fig. 6. Magnetic resonance (MR) images of a phantom prepared by the 2-stage heating of pre-soaked materials, using an oil bath of 140°C for 30 min, and then heating with that of 140°C for another 30 min while keep stirring at 120 rpm. **a**: spin-echo (SE) Image, **b**: gradient-echo (GRE) image.

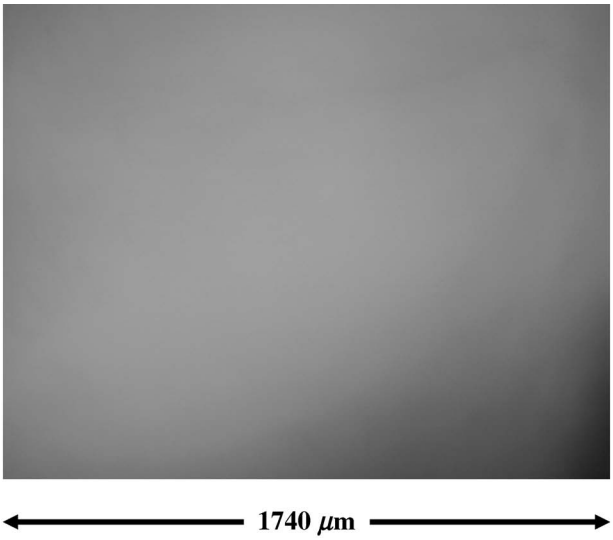

Fig. 7. Optical micrograph of phantom prepared by the 2-stage heating of pre-soaked materials, using an oil bath of 140°C for 30 min, and then heating with that of 140°C for another 30 min while keep stirring at 120 rpm. (magnification: 50 times).

Table 1. T_1 relaxation time in 5 regions of interest

Phantoms	Scan Orientations	Regions of Interest				
		O	A	B	C	D
Phantom 1	Transverse	916	909	911	909	942
	Coronal	907	855	957	899	909
	Sagittal	955	987	874	946	940
Phantom 2	Transverse	903	907	892	870	912
	Coronal	894	948	879	905	918
	Sagittal	952	883	924	955	934

(ms)

Table 2. T_2 relaxation time in 5 regions of interest

Phantoms	Scan Orientations	Regions of Interest				
		O	A	B	C	D
Phantom 1	Transverse	55	56	56	56	56
	Coronal	54	54	56	56	56
	Sagittal	54	53	56	55	56
Phantom 2	Transverse	54	57	56	57	57
	Coronal	53	52	56	55	56
	Sagittal	54	55	55	55	55

(ms)

T_2 values in 3 scan orientations at 5 ROIs in the phantom, as shown in Fig. 2.

Table 3 shows the means and standard deviations of T_1 and T_2 values measured in 2 phantoms. The T_1 value of the muscle reported in the literature is 867 ms, and the T_2 value is 47 ms.[31] The measured values in Phantom 1 were $T_1 = 921.1 \pm 33.8$ ms (mean ± standard deviation) and $T_2 = 55.3 \pm 1.0$ ms, while those for Phantom 2 were $T_1 = 911.7 \pm 26.7$ ms and $T_2 = 55.1 \pm 1.5$ ms. Deviations from the values in the literature were approximately 5% for

Table 3. Mean T_1 and T_2 values

	Phantom 1	Phantom 2	
T_1	921.1 ± 33.8	911.7 ± 26.7	N.S. $P = 0.4088$
T_2	55.3 ± 1.0	55.1 ± 1.5	N.S. $P = 0.7746$

(ms)

Notes: Results were expressed as mean ± S.D.
Statistical analysis was performed with the unpaired Student's t-test.
N.S. denotes not significant.

Table 4. Uniformity of the phantom

Indices	Phantom 1	Phantom 2	$NiSO_4$ Phantom
Maximum value (S_{max})	1,039	1,094	2,052
Minimum value (S_{min})	624	661	1,640
Span (Δ)	207.5	216.5	206.5
Median value (S)	831.5	877.5	1,846.0
Uniformity (U)	24.95	24.67	11.16

Table 5. Number of pixels containing bubbles per magnetic resonance (MR) imaging slice

Phantoms	Number of pixels	Statistics
Phantom 1	5.1 ± 7.4	N.S. $P = 0.9760$
Phantom 2	5.0 ± 8.5	

Note: Results were expressed as mean ± S.D.
Statistical analysis was performed with the Mann Whitney's U test.
N.S. denotes not significant.

T_1 values and 17% for T_2 values. Based on unpaired Student's t-test, there were no significant differences between the 2 phantoms with regard to T_1 and T_2 values (T_1 value, $P = 0.4088$; T_2 value, $P = 0.7746$).

2. Uniformity. Table 4 shows the measured indices for uniformity as described in "Experimental Methods: 2. Uniformity." Phantoms 1 and 2 show roughly the same uniformity values (U = 25%). The spherical-shaped $NiSO_4$ phantom containing aqueous solution had more uniform values than the gel phantoms (U = 11%).

3. Bubbles. Table 5 shows the average number of pixels occupied by bubbles in an MR imaging slice in 3 scan orientations. Phantom 1 had 5.1 ± 7.4 pixels/slice and Phantom 2, 5.0 ± 8.5 pixels/slice. Based on Mann-Whitney's U test, there was no significant difference in the number of pixels occupied by bubbles between the 2 phantoms ($P = 0.9760$).

Discussion

In the CAGN phantom we developed, we used 2 gelling materials as the solidifying agent and T_2 value modifier. As a result, T_1 and T_2 values equivalent to various human tissues that have high elasticity can be reproduced with the CAGN phantom. In addition, the CAGN phantom is safe for use because carrageenan, a solidifying agent, has also been used in foods. Thus, the CAGN phantom satisfies the requirements for human tissue-equivalent MR imaging phantoms.[28–31] However, the research reported has primarily comprised basic experiments using small phantoms, and the properties of larger phantoms necessary for clinical applications have not been reported. In this study, we produced and investigated the properties of columnar muscle-equivalent phantoms measuring 160 mmϕ × 100 mmh, which is suitable for scanning with a head coil.

Preparation of phantom

In our preliminary experiments, we dissolved carrageenan and agarose powders in a bath of either hot water or hot salt water. However, dissolution was poor because the temperature inside the container was inadequate for the agarose powder to dissolve completely. Although its dissolution temperature has been reported to be 90–100°C,[32] our study results indicated that agarose does not dissolve completely at temperatures slightly below 100.0°C. We could raise the temperature of the agarose mixture to 100°C by directly heating its container with a hotplate, but this scorched the gelling agent in contact with the internal surface of the container. To avoid scorching, we also attempted heating the agarose mixture using a transparent glass container heated with an infrared hotplate. Although this reduced scorching somewhat, some scorching occurred as a result of the inhomogeneity of temperature in the glass container.

In this study, we conceived the use of an oil bath for reliably raising the temperature inside the container to 100°C. When silicone oil is used, the oil bath temperature can be increased above 270°C. However, when the temperature of silicone oil becomes too high, the difference in temperatures between the oil and the mixture in the container may cause a serious problem, such as sudden spout-

ing of the oil from condensed water vapor mixing with the oil. Furthermore, heating silicone oil to 150°C or above may generate and evaporate toxic gas. Thus, it is necessary to control the temperature of the oil bath to raise the temperature inside the phantom container to 100°C in a short time while maintaining a minimal temperature difference between the inside and outside of the container. Therefore, we elected the oil bath temperature at 120°C and 140°C in our investigation. We used an enamel-coated porcelain container to avoid the dissolution of metal ions and maximize heat conduction. The capacity of the container was 3 liters to produce a phantom of 2 liters (160 mmϕ × 100 mmh). When the temperature of the oil bath was set at 120°C, temperature inside the phantom container did not reach 100°C, even after heating for 60 min. When the temperature of the oil bath was set at 140°C, the temperature inside the phantom container reached 100.0°C within 30 min. Therefore, we considered 140°C as the optimum oil bath temperature.

With regard to the dissolution of agarose, we compared the outcomes of direct dissolution (using powder-form ingredients) and 2-stage heating with pre-soaked materials (post-swelling dissolution using liquid-form ingredients, soaking them in water overnight). Using the direct dissolution method, we observed numerous agar clusters and bubbles on MR images and optical micrographs, indicating poor dissolution. Placing a mixture of agarose and carrageenan powder into the hot water generated numerous masses with gelatinous surfaces. High-concentration gel films on the surfaces of these masses prevented water from penetrating into the masses, which resulted in poor dissolution. It is also likely that bubbles within the masses caused insufficient bubble elimination. Therefore, the agarose and carrageenan were each soaked in water and swollen one day before dissolution, which helped avoid clustering. However, numerous bubbles generated by boiling remained in the phantom, trapped in the solution as a result of its high viscosity. In addition, the solution sometimes bubbled over into the high-temperature oil bath and steam vaporized. Complete dissolution of agarose required heating the solution to 100°C, but this increased viscosity and generated bubbles. This problem was resolved by introducing the 2-stage heating method using an oil bath.

It has been known that the dissolution temperature of agarose is 90–100°C, and its gelling temperature is 40°C. However, the results of this study indicated that the temperature for complete dissolution of agarose is 100.0°C, which is very difficult to achieve. On the other hand, the dissolution temperature of carrageenan is about 70°C, and its gelling temperature is 60°C.[32,33] Therefore, we devised a 2-stage heating method in which agarose was completely dissolved at 100.0°C and carrageenan was then added. With these considerations, we boiled the agarose solution in the enamel-coated porcelain container for 30 min and dissolved it completely using the oil bath at 140°C, then added water containing swollen carrageenan at room temperature. After a total of 60 min heating and stirring, complete dissolution and degassing were achieved.

We previously tried degassing using a vacuum pump, vacuum container, and plate heater to eliminate bubbles. However, the temperature of the solution dropped with this method; in addition, bubbles in the phantom were thought to be due to steam rather than air. Thus, we decided not to employ such a method.

On MR images and optical micrographs, we observed no clusters from poor dissolution in the phantoms prepared by the 2-stage heating method using pre-soaked materials. Carrageenan gel has been known to become brittle after prolonged heating, but in the 2-stage heating method, carrageenan is added later, thus minimizing duration of heating and retaining material stability. With MR imaging, we observed no bubbles on SE images but a number of small bubbles on GRE images. We used GRE to detect bubbles because of its sensitivity to differences in magnetic susceptibility. At approximately 100°C, agarose and carrageenan are in a sol state with low viscosity. However, the gelation temperature of carrageenan is 60°C, which is relatively high. With natural cooling, the viscosity of the solution increases as temperature decreases, and small bubbles would remain in the phantom.

Properties of phantoms with 2-stage heating method using pre-soaked materials

We made two 2-liter muscle-equivalent phantoms on separate days by combining the post-swelling dissolution method with the 2-stage heating method. Because of weight loss of solution by evaporation during heating, we adjusted the amount of water to make a phantom weighing 2,000 g.

We evaluated the 2 phantoms by MR imaging. There were no significant differences in T_1 and T_2 values (Table 3); uniformities (U) were similar (Table 4); and there was no significant difference in the amount of bubbles between the 2 phantoms (Table 5). Both phantoms had mean bubble amounts of fewer than 10 pixels/slice. Our preparation method for clinically suitable phantoms is considered optimum for uniformity and reproduci-

bility.

Comparing the relaxation times between the muscle tissue-equivalent portion of our phantom and those of reported clinical data in the literature, the prepared phantoms had approximately 5% higher T_1 values and 17% higher T_2 values. This would result from deterioration of $GdCl_3$ over time. Our preliminary experiment results showed that a $GdCl_3$ solution tended to degenerate over time. A drawback of our study was that the maximum size of the MR imaging phantom was limited by the size of the oil bath (293 mm × 340 mm × 270 mm).

In SE sequence, although a flip angle of 90 degrees is generally used as a parameter for MR imaging, we used a flip angle of 70 degrees, which has been used for clinical evaluation in our institution. In GRE sequence, we applied parameters we use for detecting hemorrhagic lesions. Using the clinical scanning parameters, we could clearly observe the difference in uniformity between the direct dissolution (lack of uniformity) and 2-stage heating (uniformity) methods; thus we employed the parameters for clinical evaluation.

In the present study, which considers the clinical utilization of an MR imaging phantom, we employed the parameters used in our institution for detecting cerebral hemorrhage to evaluate the ratio of bubbles in the phantom. Although the magnetic susceptibility in the regions of bubbles and that in hemorrhage are different, MR imaging evaluation is frequently applied for such case.

In recent years, stent therapy with non-magnetic metals has become increasingly common. MR imaging is often performed on patients having implanted stents. The image artifacts caused by non-magnetic metals on MR imaging are minor in comparison with those caused by magnetic metals; however, because the stents conduct electricity, variable magnetic fields induce electric currents at a stent. The present phantom is thus considered useful for investigating how MR image quality is affected by such electric currents because its conductivity can be adjusted according to experimental requirements.

Conclusion

Optimum heating preparation for uniform and reproducible phantoms was achieved by combining the post-swelling dissolution and the 2-stage heating methods with a silicone oil bath. Future applications of a human tissue-equivalent MR imaging phantom, our CAGN phantom, produced by our method, can serve investigations of MR imaging phenomena that cannot be performed on the human body.

Acknowledgements

This work was supported in part by Grants in Aid for Scientific Research from the Ministry of Education, Culture, Sports Science and Technology, Japan (#15209063, #19591418).

References

1. Kjaer L, Thomsen C, Henriksen O, Ring P, Stubgaard M, Pedersen EJ. Evaluation of relaxation time measurements by magnetic resonance imaging. A phantom study. Acta Radiol 1987; 28:345–351.
2. Kjaer L, Thomsen C, Larsson HB, Henriksen O, Ring P. Evaluation of biexponential relaxation processes by magnetic resonance imaging. A phantom study. Acta Radiol 1988; 29:473–479.
3. Mathur-De Vre R, Grimee R, Parmentier F, Binet J. The use of agar gel as a basic reference material for calibrating relaxation times and imaging parameters. Magn Reson Med 1985; 2:176–179.
4. Mitchell MD, Kundel HL, Axel L, Joseph PM. Agarose as a tissue equivalent phantom material for NMR imaging. Magn Reson Imaging 1986; 4: 263–266.
5. Lutz NW, Schultz E. Phantom material for quantitative evaluation of MR images. Med Prog Technol 1986; 11:177–184.
6. Kraft KA, Fatouros PP, Clarke GD, Kishore PR. An MRI phantom material for quantitative relaxometry. Magn Reson Med 1987; 5:555–562.
7. Howe FA. Relaxation times in paramagnetically doped agarose gels as a function of temperature and ion concentration. Magn Reson Imaging 1988; 6:263–270.
8. Bucciolini M, Ciraolo L, Lehmann B. Simulation of biologic tissues by using agar gels at magnetic resonance imaging. Acta Radiol 1989; 30:667–669.
9. Groch MW, Urbon JA, Erwin WD, al-Doohan S. An MRI tissue eqivalent lesion phantom using a novel polysaccharide material. Magn Reson Imaging 1991; 9:417–421.
10. Christoffersson JO, Olsson LE, Sjöberg S. Nickel-doped agarose gel phantoms in MR imaging. Acta Radiol 1991; 32:426–431.
11. Tofts PS, Shuter B, Pope JM. Ni-DTPA doped agarose gel–a phantom material for Gd-DTPA enhancement measurements. Magn Reson Imaging 1993; 11:125–133.
12. Mazzara GP, Briggs RW, Wu Z, Steinbach BG. Use of a modified polysaccharide gel in developing a realistic breast phantom for MRI. Magn Reson Imaging 1996; 14:639–648.
13. Luft AR, Skalej M, Welte D, Kolb R, Klose U. Re-

liability and exactness of MRI-based volumetry: a phantom study. J Magn Reson Imaging 1996; 6: 700–704.
14. Shapiro EM, Borthakur A, Reddy R. MR imaging of RF heating using a paramagnetic doped agarose phantom. MAGMA 2000; 10:114–121.
15. Chen ZJ, Gillies GT, Broaddus WC, et al. A realistic brain tissue phantom for intraparenchymal infusion studies. J Neurosurg 2004; 101:314–322.
16. Madson EL, Fullerton GD. Prospective tissue-mimicking materials for use in NMR imaging phantoms. Magn Reson Imaging 1982; 1:135–141.
17. Tsuruda JS, Bradley WG. MR detection of intracranial calcification: a phantom study. AJNR Am J Neuroradiol 1987; 8:1049–1055.
18. Blechinger JC, Madsen EL, Frank GR. Tissue-mimicking gelatin-agar gels for use in magnetic resonance imaging phantoms. Med Phys 1988; 15: 629–636.
19. Baird DK, Kincaid SA, Hathcock JT, Rumph PF, Kammerman J, Visco DM. Effect of hydration on signal intensity of gelatin phantoms using low-field magnetic resonance imaging: possible application in osteoarthritis. Vet Radiol Ultrasound 1999; 40: 27–35.
20. Mano I, Goshima H, Nambu M, Iio M. New polyvinyl alcohol gel material for MRI phantoms. Magn Reson Med 1986; 3:921–926.
21. Chu KC, Rutt BK. Polyvinyl alcohol cryogel: an ideal phantom material for MR studies of arterial flow and elasticity. Magn Reson Med 1997; 37: 314–319.
22. Lukas LA, Surry KJ, Peters TM. Temperature dosimetry using MR relaxation characteristics of poly(vinyl alcohol) cryogel (PVA-C). Magn Reson Med 2001; 46:1006–1013.
23. Surry KJ, Austin HJ, Fenster A, Peters TM. Poly-(vinyl alchol) cryogel phantoms for use in ultrasound and MR imaging. Phys Med Biol 2004; 49: 5529–5546.
24. De Luca F, Maraviglia B, Mercurio A. Biological tissue simulation and standard testing material for MRI. Magn Reson Med 1987; 4:189–192.
25. Howe FA, Griffiths JR. A two-compartment phosphate-doped gel phantom for localized spectroscopy. Magn Reson Imaging 1992; 10:119–126.
26. Vitkin IA, Moriarty JA, Peters RD, et al. Magnetic resonance imaging of temperature changes during interstitial microwave heating: a phantom study. Med Phys 1997; 24:269–277.
27. Goldstein DC, Kundel HL, Daube-Witherspoon ME, Thibault LE, Goldstein EJ. A silicone gel phantom suitable for multimodality imaging. Invest Radiol 1987; 22:153–157.
28. Yoshimura K, Kato H, Kuroda M, et al. Development of a tissue-equvalent MRI phantom using carrageenan gel. Magn Reson Med 2003; 50:1011–1017.
29. Kato H, Yoshimura K, Kuroda M, et al. Development of a phantom compatible for MRI and hyperthermia using carrageenan gel–relationship between dielectric properties and NaCl concentration. Int J Hyperthermia 2004; 20:529–538.
30. Yoshida A, Kato H, Kuroda M, et al. Development of a phantom compatible for MRI and hyperthermia using carrageenan gel–relationship between T_1 and T_2 values and NaCl concentration. Int J Hyperthermia 2004; 20:803–814.
31. Kato H, Kuroda M, Yoshimura K, et al. Composition of MRI phantom equivalent to human tissues. Med Phys 2005; 32:3199–3208.
32. Osada Y, Kajiwara K. Gels Handbook. Tokyo, Japan: New Technology New Science, 1997; 735. (Japanese)
33. Osada Y, Kajiwara K. Gels Handbook. Tokyo, Japan: New Technology New Science, 1997; 743–744. (Japanese)
34. National Electric Manufacturers Association: Determination of image uniformity in diagnostic magnetic resonance images. USA: NEMA Standard Publication, 1989; MS3.